



# SRF



## **Radiation hardness tests of piezoelectric actuators with fast neutrons at liquid helium temperature**

M. Fouaidy<sup>1</sup>, G. Martinet<sup>1</sup>, N. Hammoudi<sup>1</sup>, F. Chatelet<sup>1</sup>, A. Olivier<sup>1</sup>, S. Blivet<sup>1</sup>, F. Galet<sup>1</sup>

CNRS-IN2P3-IPN Orsay, France

### **Abstract**

Piezoelectric actuators, which are integrated into the cold tuning system and used to compensate the small mechanical deformations of the cavity wall induced by Lorentz forces due to the high electromagnetic surface field, may be located in the radiation environment during particle accelerator operation. In order to provide for a reliable operation of the accelerator, the performance and life time of piezoelectric actuators (~24.000 units for ILC) should not show any significant degradation for long periods (i.e. machine life duration: ~20 years), even when subjected to intense radiation (i.e. gamma rays and fast neutrons). An experimental program, aimed at investigating the effect of fast neutrons radiation on the characteristics of piezoelectric actuators at liquid helium temperature (i.e.  $T \sim 4.2$  K), was proposed for the working package WP#8 devoted to tuners development in the frame of CARE project. A neutrons irradiation facility, already installed at the CERI cyclotron located at Orléans (France), was upgraded and adapted for actuators irradiations tests purpose. A deuterons beam (maximum energy and beam current: 25 MeV and  $35 \mu\text{A}$ ) collides with a thin (thickness: 3 mm) beryllium target producing a high neutrons flux with low gamma dose (~20%): a neutrons fluence of more than  $10^{14}$  n/cm<sup>2</sup> is achieved in ~20 hours of exposure. A dedicated cryostat was developed at IPN Orsay and used previously for radiation hardness test of calibrated cryogenic thermometers and pressure transducers used in LHC superconducting magnets. This cryostat could be operated either with liquid helium or liquid argon. This irradiation facility was upgraded for allowing fast turn-over of experiments and a dedicated experimental set-up was designed, fabricated, installed at CERI and successfully operated for radiation hardness tests of several piezoelectric actuators at  $T \sim 4.2$  K. This new apparatus allows on-line automatic measurements of actuators characteristics and the cryogenic parameters. Further, the test-cell and actuators are equipped with high purity Ni foils for measuring the total neutrons dose by an activation method. In this report, the details of the irradiation test facility will be described then the experimental data will be analyzed and discussed.



The internal diameter and available height for the cryogenic liquid (i.e., helium or argon) vessel are respectively 200 mm and 640 mm. The vacuum vessel and the parts of the insert located in the neutrons beam region are made of aluminium to avoid material activation. Note that the argon condenser, which is not used for the actual liquid helium tests, was removed. Due to the relatively small available space in front of the beam line, we have designed and installed a handling system (Fig. 2) consisting of a support sliding in a horizontal rail. This system allows the following operation: a) moving easily and rapidly the cryostat, b) positioning the cryostat and adjusting the location of the test-cell in front of the beam line.

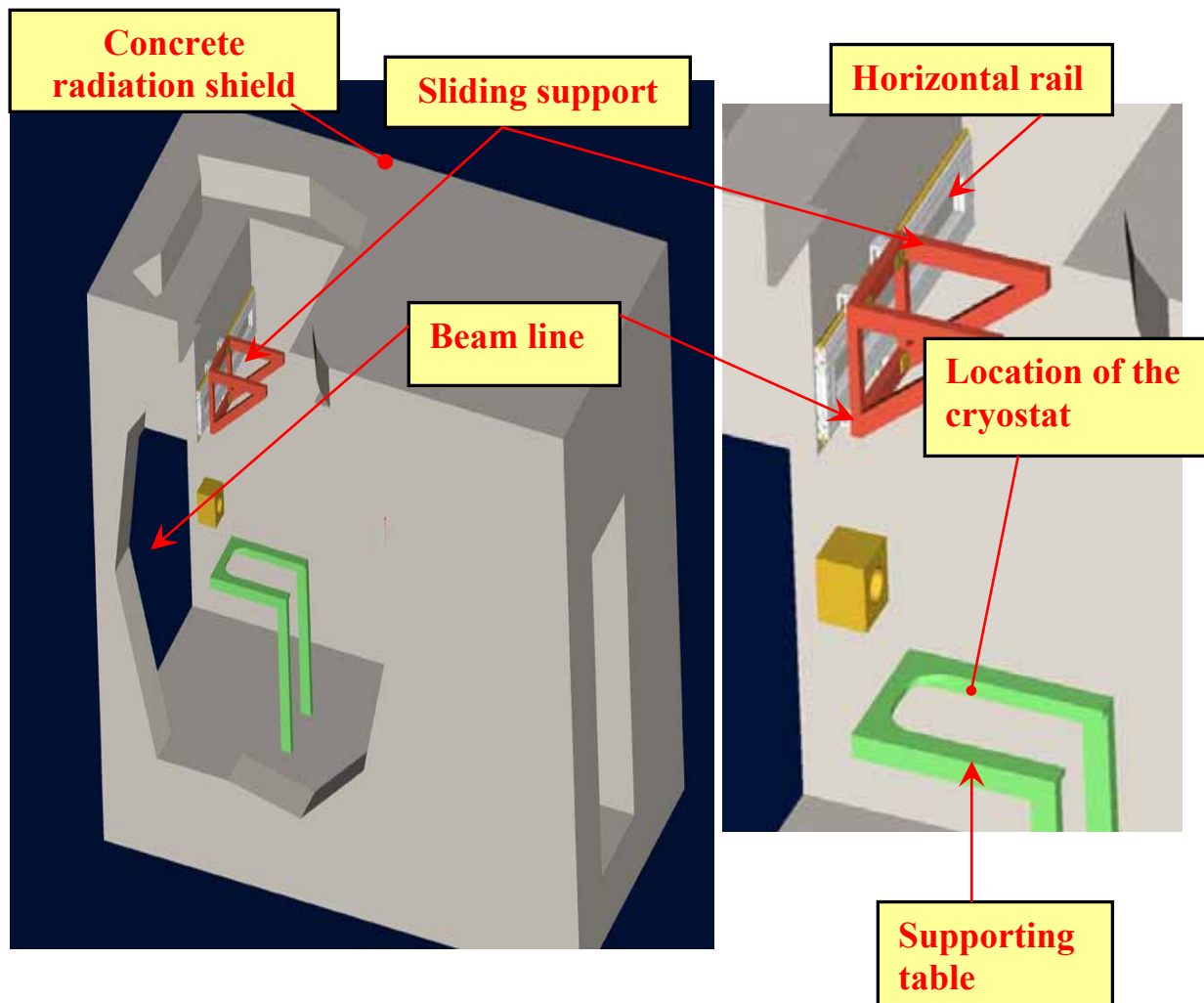


**Fig. 2: 3D view of the cryostat handling system in front of the beam line.**

The actuators to be simultaneously irradiated (up to four) are housed in vacuum can, which is immersed in a liquid helium bath for low temperature ( $T \sim 4.2$  K) experiments. The cryostat is placed behind a 3 mm thick beryllium target located at a distance  $d = 20$  mm - 30 mm from the cryogenic vessel. The high flux of neutrons is produced (Fig. 3) by the collision of a deuterons beam (maximum energy and intensity: 25 MeV and  $35 \mu\text{A}$  respectively) with the beryllium target using the break-up reaction  ${}^9\text{Be}(d, n){}^{10}\text{B}$ . Note that the target is water-cooled (forced convection) in order to avoid strong heating of the material. A more detailed description of the neutrons production is presented in a next section.

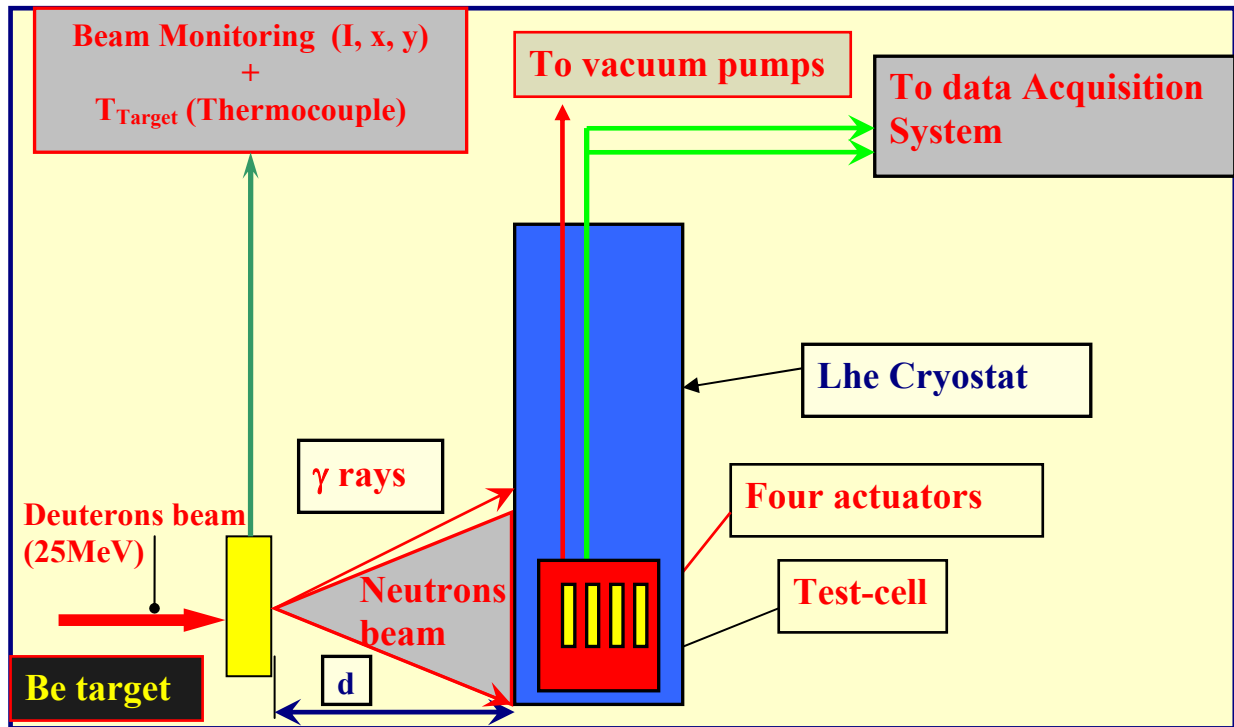


**Fig. 3: Sketch of fast neutrons production process.**

## Description of the experimental set up

### The test-cell

As the actuators will not operate in the same conditions as the LHC thermometers, a new insert was developed for actuator irradiations tests. In fact, for their operation in the fast cold tuning system of SRF cavities, the actuators are located in the insulation vacuum of the cryomodule and consequently are not directly cooled by superfluid helium. The main design requirements of the test-cell are listed in Table 1.

Component, parameter (Unit)	Design value- Material
All component in cold area	<b>Suitable for operation in radiation and cryogenic environment</b>
Chamber and actuator support	<b>Aluminium</b>
Temperature range (K)	<b>4.2 -300</b>
Pressure in the chamber (Torr)	<b>&lt;10<sup>-6</sup></b>
Irradiated area (mm <sup>2</sup> )	<b>&gt;80x40</b>
Liquid Helium Pressure (Bar)	<b>1</b>
Liquid Helium Temperature (K)	<b>4.2 K</b>
Low temperature vacuum seals	<b>Demountable indium gasket</b>
Pumping speed in the tube (l/s)	<b>0.05</b>
Leak rate at T=300 K (mBar.l.s <sup>-1</sup> )	<b>&lt;10<sup>-9</sup></b>
Pumping time from 10 <sup>-2</sup> Torr to 10 <sup>-6</sup> Torr (min.)	<b>&lt;10</b>

**Table 1: Design requirements of the irradiations test-cell**

The test-cell (Fig .4), which is made of aluminium, consists mainly of a mechanical support for the actuators and a vacuum chamber with a vertical (I.D:16 mm) pumping line. The actuators are housed into the aluminium support, which is inserted in the vacuum chamber. The main dimensions of the test cell are: 1) internal diameter: 100mm, 2) actuator supports outer diameter: 160mm. A high purity indium gasket is placed in a groove machined in the actuators support to insure the vacuum-tightness between the evacuated chamber and the surrounding Liquid Helium (LHe) bath. Note that a high purity (>99.99%) indium (wire diameter: 1 mm) was used in order to reduce material activation due to exposure to radiation. Moreover, the pumping tube has two other functions: 1) feed through for all the wires attached to the actuators, 2) mechanical support attaching the test-cell to the cryostat insert. Each of the 4 piezoelectric actuators to be tested is equipped with a calibrated (1.5 K-300 K) resistive Allen-Bradley thermometer. The Allen-Bradley thermometers were chosen according to several criteria: 1) they feature good sensitivity and precision in the temperature range of interest, 2) they are suited for use in radiation environment [7-9] and the effect of fast neutrons on their thermometric characteristics is well-known.

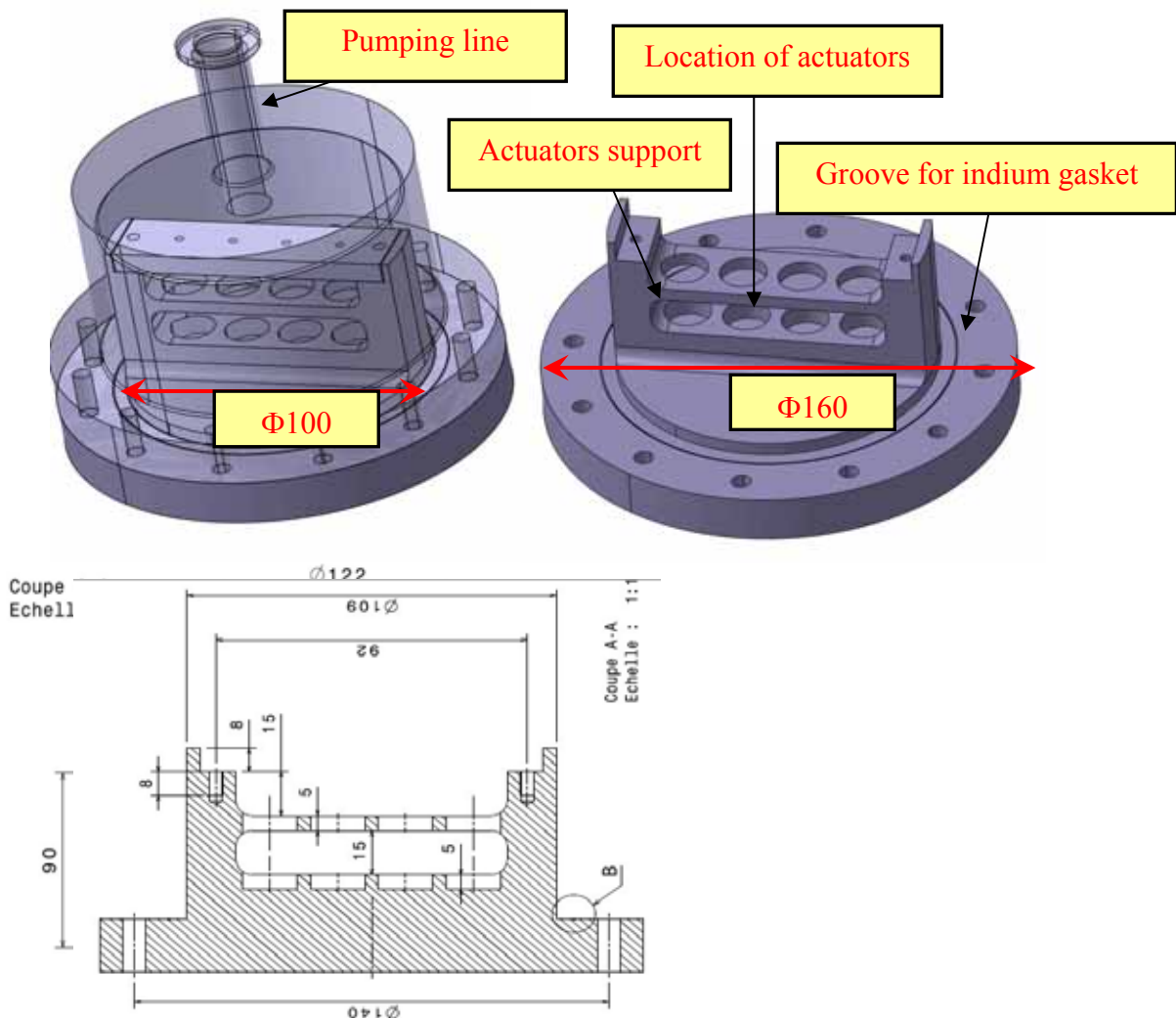


**Fig. 4. Drawings of the test chamber**

The piezostacks are inserted into their fixture and mounted with a copper-beryllium spring on their upper extremity. Moreover, an indium foil is sandwiched between the actuator lower extremity and the support in order to improve the thermal contact. Further a heater and a copper thermal anchor are attached to each actuator.

## Pumping system design

As the overall conductance of the pumping circuit is mainly dominated by the conductance  $C$  of the pumping tube of the cryostat insert, we have calculated the variations of this parameter as function of the tube diameter  $d$  (Fig. 5). These results show that tube with 16mm internal diameter have a conductance  $\sim 9$  times higher than the design value with a good safety margin. Note that as the pumping tube is used for the passage of the 32 instrumentation wires for the 4 actuators, the effective diameter is much lower than the nominal value  $d=16\text{mm}$ .

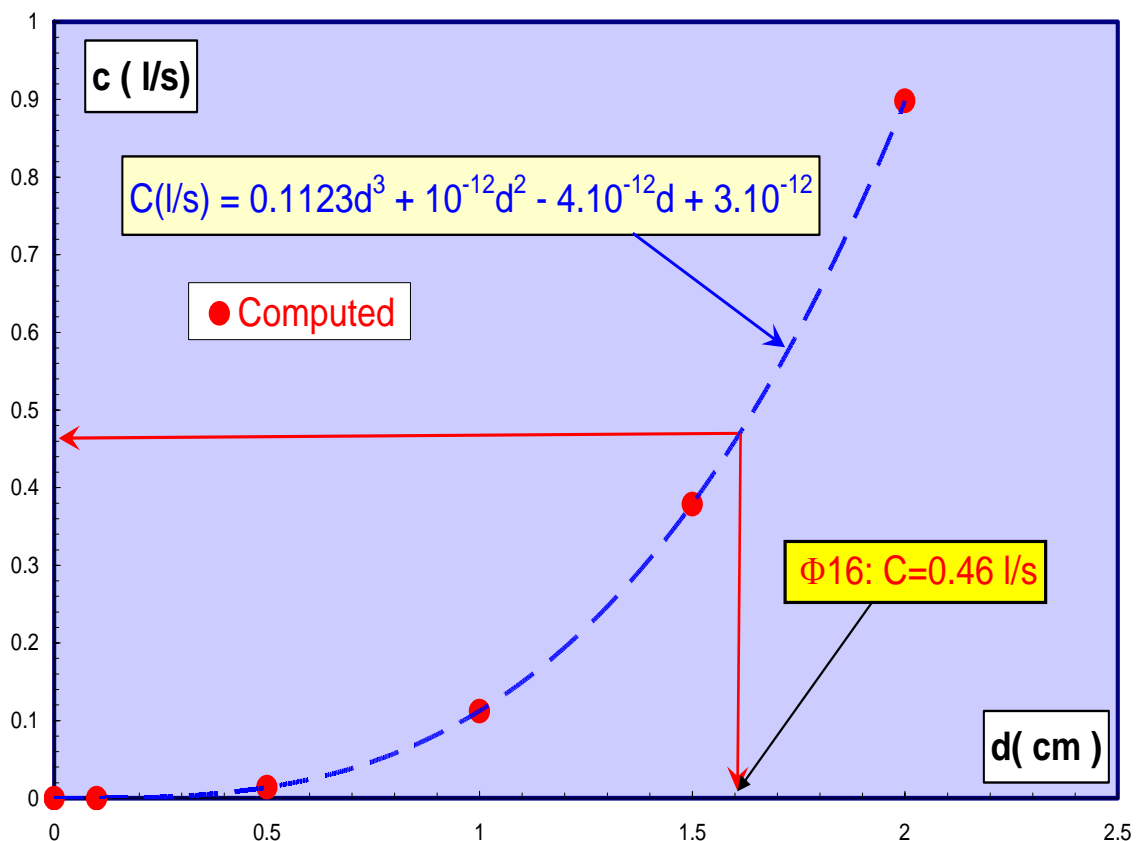


**Fig. 5: Conductance of the pumping line versus tube diameter (tube length = 1085 mm)**

Further, the theoretical time required for the removal of air in the chamber in the Knudsen regime (i.e., initial and final pressure:  $10^{-2}$  and  $10^{-6}$  Torr respectively) was computed as function of  $d$  (Fig. 6). Note that in our calculations of pumping duration, the out-gassing (i.e., desorption) of gases from the inner surfaces of the system was not taken into account. Consequently, the effective duration of pumping the system should be much higher.

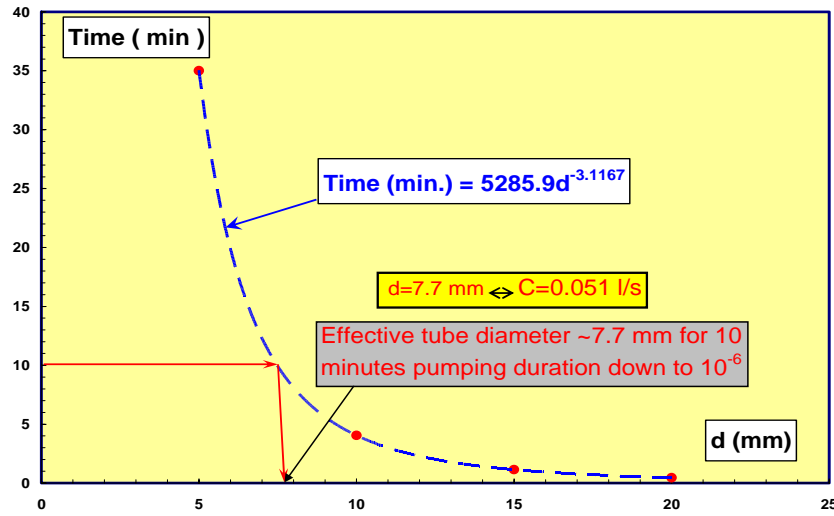


**Fig. 6: Pumping duration of the test-cell in the Knudsen regime for reducing the pressure from  $10^{-2}$  to  $10^{-6}$  Torr (Material desorption not taken into account).**

The results lead to an effective tube diameter of ~8 mm to fulfil the test-cell vacuum requirements.

### Wiring for the actuators and sensors

In order to avoid parasitic and contact impedances due to wiring, all the measurements (actuator impedance, thermometer signals,...) were performed using the four probe technique. Moreover, for reliability reasons and intense radiations environment compatibility, the standard low temperature feed through (e.g., glass-metal junction mounted on a stainless flange) could not be used in our apparatus. Consequently, the pumping tube is used for the passage of all the 32 wires (4 actuators and 4 Allen Bradley thermometers). Moreover, in order to save space and allow a sufficient effective diameter (pumping time reduction) of the pumping tube, we used four twisted manganin wires (diameter: 0.125 mm, electrical resistivity:  $\rho_e=47.10^{-8}\Omega.m$ ) to reduce the conduction heat flux from room temperature ( $T=300K$ ) to the actuators ( $T\sim 4.2 K$ ). It is then necessary to compute the temperature profile along these wires and the resulting conduction heat flux at their cold extremity. As the wires are under vacuum, there is no radial heat flow to the surroundings. In steady state regime, the resulting one directional heat transport in the wires is governed by the well-known heat equation:

$$\frac{d^2T}{dz^2} + \left(\frac{\rho_e}{k}\right) \cdot j^2 = 0 \quad (1)$$

In the above equation,  $j$  and  $k$  are respectively the current density in the wire and the thermal conductivity of the material. The two extremities of the wire are respectively maintained at  $T_H=300 K$  and  $T_C=4.2 K$  leading to the following boundary conditions:  $T=300 K$  at  $z=0$  and  $T=4.2 K$  at  $z=L$  ( $L=1500 mm$  is the wire length). The temperature profile along the wire is parabolic:

$$T(z^*) = A \cdot z^{*2} + B \cdot z^* + C \quad (2)$$

With:

$z^* = z/L$  : reduced coordinate

$$A = - \left( \frac{\rho_e}{k} \right) \cdot j^2 \tag{3}$$

$$B = T_C - T_H + \frac{K \cdot L^2}{2} \tag{4}$$

$$C = T_H \tag{5}$$

The resulting temperature profiles for the thermometer wire (sensing current:  $I=10 \mu\text{A}$ ) and actuator wire (sensing current:  $I=1.67\text{mA}$ ) are presented in Fig. 7. As expected, the results show that the Joule heating which is negligible (i.e.,  $|A| = 2.64 \cdot 10^{-2} \text{ K}$  and  $|B| = 295.8 \text{ K}$ ) in the case of thermometer sensor wires, leading to a quasi linear temperature profile. In contrast, for the actuator wires the Joule heating, which is much more important (i.e.,  $|A| = 736 \text{ K}$  and  $|B| = 440 \text{ K}$ ) has an observable effect leading to a parabolic temperature profile.

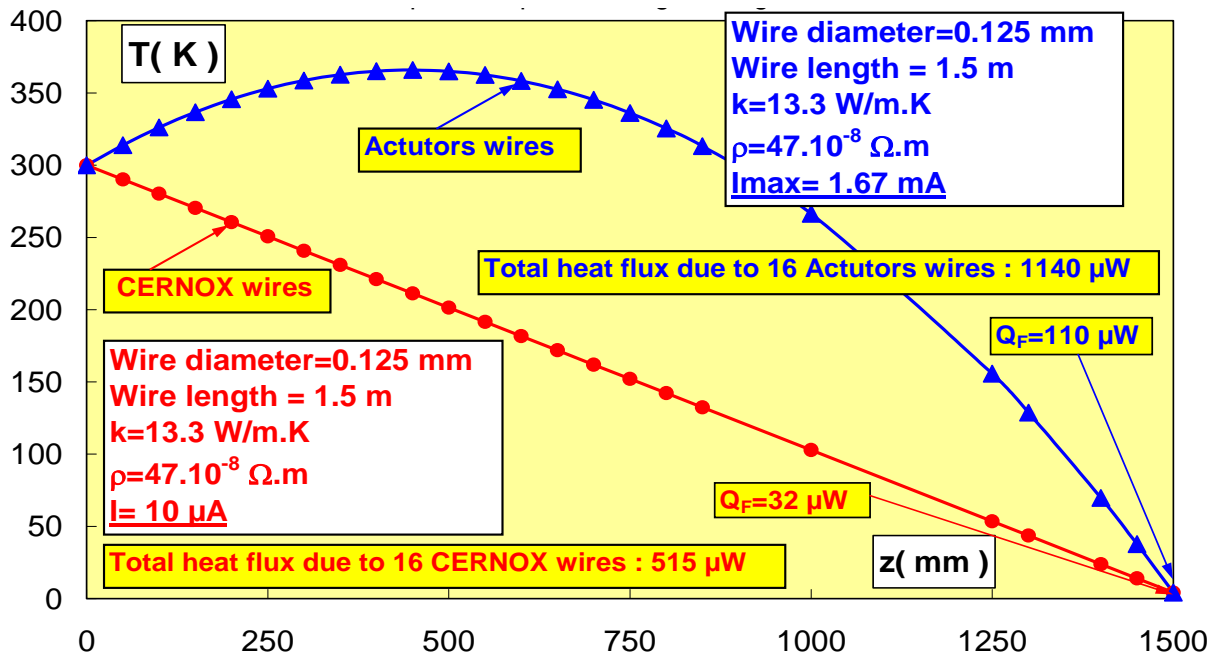


**Fig. 7: Temperature profile along the manganin wires ( Actuators and CERNOX).**

Moreover, from these results we calculated the conduction heat flux at the thermometer cold extremity and we obtained  $Q_F=32 \mu\text{W}$ : the total heat flux for the  $4 \times 4$  wires of the thermometers is then  $Q_T=515 \mu\text{W}$ . For the actuator current wire ( $I_{\text{max}}=1.67\text{mA}$ ),  $Q_F=110 \mu\text{W}$ : the total heat flux for the  $4 \times 4$  wires of actuators is then  $Q_T=1140 \mu\text{W}$ . The total heat flux due to all these wires is then  $1.7 \text{ mW}$  ( $425 \mu\text{W}$  per actuator). It must be stressed that, in order to reduce significantly (e.g., two orders of magnitude) the heat flux at  $4.2 \text{ K}$ , twisted manganin wires were used instead of usual copper based coaxial cables for the wiring of the actuators. Notice that the pumping tube acts as a shielding against electromagnetic perturbations for the low level signals ( $0.2 \text{ mV}$ - $10 \text{ mV}$ ) of the thermometers.



## The piezoelectric actuators tested

Three types of low voltage multilayer piezostacks supplied by 3 different companies were subjected to irradiation tests namely 4 NOLIAC actuators from NOLIAC Company, 4 PICMA actuators from PI, and 3 Piezosystem JENA actuators. The main electromechanical properties of these actuators are illustrated in Table 2. The irradiation tests data concerning Piezosystem JENA piezostacks will be not included in this report. These actuators were tested for historical reasons (first actuators used in the cold tuner of TTF cavities), but they are not good candidate for the tuner: their life time is very short at cryogenic temperature. Note that three to four actuators of each type were tested simultaneously to improve the statistics.

Supplier	NOLIAC	Physik Instruments	Piezosystem JENA
Parameter (unit)			
Type-Material	PZT- pz27	PICMA- PZT 25	PZT
Length (mm)	30	35	42
Section (mm <sup>2</sup> )	10x10	10x10	5x5
Young Modulus (GPa)	45	37	50
Nominal displacement at T~300K (μm)	42	35	40
Natural Frequency (kHz)	66	40	N.A
Stiffness (N/μm)	150	105	25
Blocking force (kN)	6.3	3.6	1
Capacitance @300 K (μF)	5.7	12.4	3.4
Maximum voltage (V)	200	120	150

**Table 2: Main electromechanical properties of the actuators irradiated.**

## Neutrons spectrum and irradiation calculations

The material used for the construction of the cryostat insert should be suitable for operation in radiation and low temperature environment. Hence it should be chosen according to activity considerations and cryogenic performance (e.g., low thermal conduction). More precisely the activations of the following materials were calculated: 1) indium for gasket, 2) aluminium for vacuum chamber, actuator support and pumping line, 3) other materials (screws, nuts, ...). The maximum energy  $E_{\max}$  and intensity  $I_{\max}$  of the deuterons beam delivered by the CERI cyclotron are respectively 25 MeV and 35 μA. Further, the envelop size of the beam is 5x5 mm<sup>2</sup>. The neutrons are produced by the collision of the deuterons beam with a 5 cm thick beryllium target located in front of the cryostat: the resulting distance between beryllium target and actuators support is in the range 15cm-30 cm. The neutrons production process is based on the break-up reaction  ${}^9\text{Be}(d, n){}^{10}\text{B}$ .

## Neutrons spectrum

The expected spectrum of these neutrons will be similar (homothetic) to that obtained with SARA facility [6] with a magnification due to the differences in the values of the maximum energy of the deuterons beam ( $E_{\max} = 25$  MeV for CERI facility,  $E_{\max} = 21$  MeV for SARA facility). This approximation is confirmed by the work of Parnell [10] and Maunoury [11]. Maunoury showed that the mean energy  $\langle E_{\text{neutrons}} \rangle$  of the neutrons spectrum in the beam direction increases linearly with the deuteron energy  $E_d$  according to the following empirical relation ship:

$$\langle E_{\text{neutrons}} \rangle = 0.38E_d + 0.57 \quad (6)$$

The expected spectrum is calculated by using the spectrum measured at SARA facility which is interpolated for a 25 MeV deuteron beam and normalised at the integrated dose.

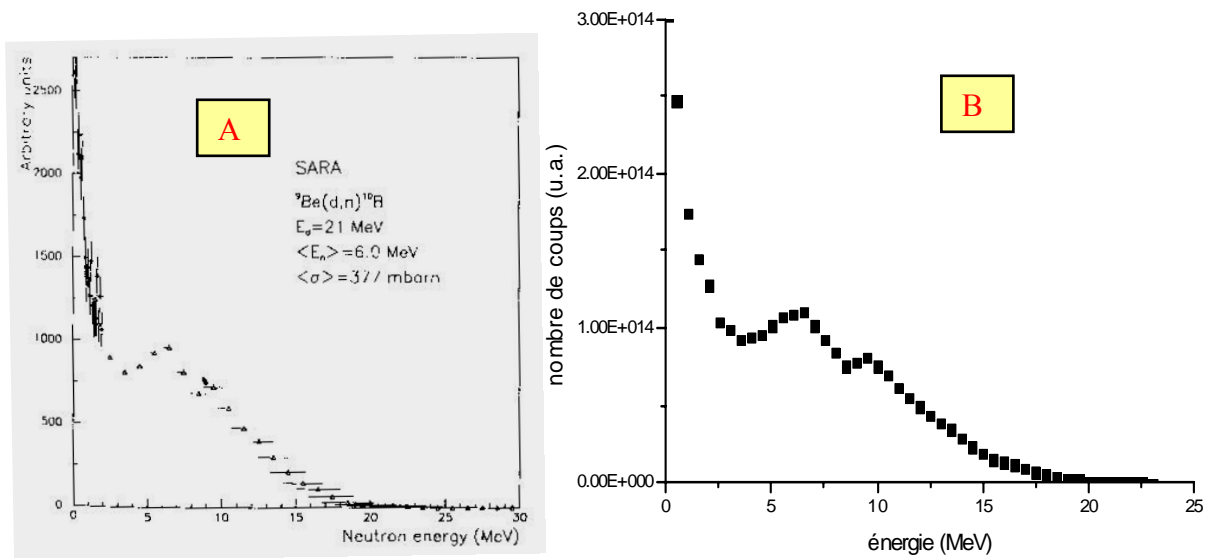


**Fig. 8: Measured (A) and computed (B) neutrons spectrum (SARA facility)**

The computed neutrons spectrum (Fig. 8 B) is in very good agreement with the experimental data (Fig. 8 A) obtained previously with for SARA facility [6] at a maximum deuterons energy  $E_{\max} = 21$  MeV. Consequently, we can use with a high confidence the simulated neutrons spectrum in the case of the CERI facility ( $E_{\max} = 25$  MeV).

Finally, the number of activated atoms  $N$  at the neutron energy  $\varepsilon$  is calculated using the well-known formulae:

$$N(\varepsilon) = \Phi(\varepsilon) \cdot \frac{m \cdot N_A}{M} \cdot \sigma(\varepsilon) \quad (7)$$

Where  $\Phi$  is the neutrons flux (neutrons/cm<sup>2</sup>),  $m$  the target thickness (g),  $N_A$  the Avogadro number,  $M$  the molar mass and  $\sigma(\epsilon)$  the cross section of the reaction at the energy  $\epsilon$ .

According to previous experiment, the integrated neutron dose expected at 8.5 cm from target with a deuteron beam of 21 MeV and 7  $\mu$ A is above 0.9 à 1.9.10<sup>15</sup> n/cm<sup>2</sup> after an exposure time of 20 hours. Regarding the actual setup (20 cm, 35  $\mu$ A, 23 MeV, 8 hours), the expected dose is in the range 0.32.10<sup>15</sup>-0.7.10<sup>15</sup> neutrons/cm<sup>2</sup>.

## Material activation

The cross sections are taken from the nuclear data base ENDF and calculations were focused only on the following reactions for the indium activation coming from the gasket of the test cell:  $^{115}\text{In}(n,\gamma)^{116}\text{In}$ ,  $^{115}\text{In}(n,2n)^{114}\text{In}$ ,  $^{115}\text{In}(n,p)^{115}\text{Cd}$ ,  $^{115}\text{In}(n,\alpha)^{112}\text{Ag}$ . Due to the short decay period and the rather low cross section and/or neutron flux in the energy range of interest, most of the above reactions don't produce high activation ten days after irradiation experiment. In contrast,  $^{115}\text{In}(n,2n)^{114}\text{In}$  and  $^{115}\text{In}(n,p)^{115}\text{Cd}$  reactions could induce enough activation: indeed the decay periods of the first excited states of  $^{114}\text{In}$  and  $^{115}\text{Cd}$  are respectively ~49 and ~45 days. In the worst case, if all produced nucleus are excited, it induces respectively an activity above 600 kBq and 4 kBq ten days after irradiation. These results were confirmed by the tests: no significant activity has been detected from indium after irradiation experiment.

## Neutron fluence measurements

### Principle of nickel foils activation

The neutron fluences received by the actuators during irradiations are measured by means of an activation method of nickel foils which are attached the tested actuators support using a Kapton film (Fig. 9).

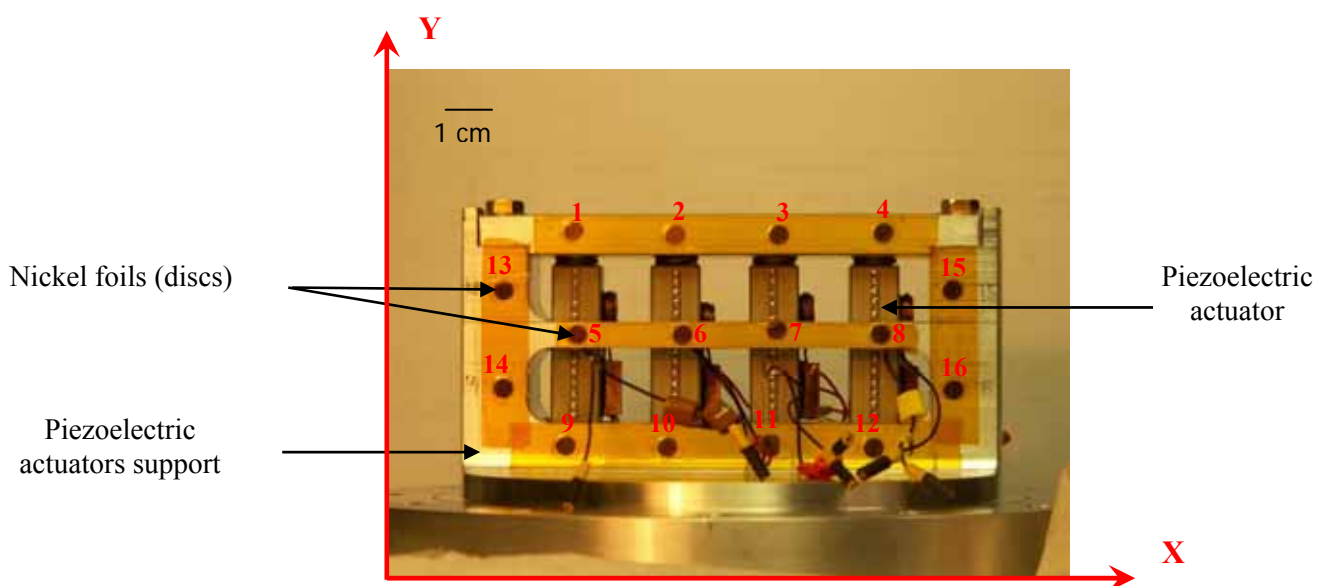


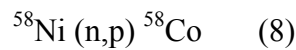
**Fig. 9: Locations of the nickel foils on the PICMA piezoelectric actuators support**

The main characteristics of these nickel foils supplied by Goodfellow are summarized in Table 3.

Diameter (mm)	Thickness (mm)	Mass (mg)	Purity of Ni (%)
4	0.125	14.4	99.999

**Table 3: Values of the main characteristics of the nickel foils**

The activation method is based on the charge exchange reaction on  $^{58}\text{Ni}$  :



The determination of the nickel foils activity is performed by  $\gamma$  rays spectrometry: we measure (Fig. 10) the gamma ray of  $^{58}\text{Co}$  at 810 keV by means of a liquid nitrogen cooled (T=77K) ORTEC Ge-Li detector (Table 4).

Trademark	ORTEC
Type	8011-10185
Diameter of the crystal	43 mm
Length of the crystal	51.5 mm
Voltage	+ 4800 V
Resolution (FWHM) @ 1.33 MeV	1.77 keV
Relative efficiency	11.4%
Resolution @ 122 keV	1.08 eV

**Table 4: Characteristics of the Ge-Li detector**



**Fig.10: Gamma spectroscopy apparatus (detector and data acquisition system)**

A close view photograph of the detector with lead shielding is shown in Fig. 11.



**Fig. 11: The detector with its Pb shielding**

The resulting nickel activity  $A_{Ni}$  (Fig. 12) is then used for calculating the neutrons fluence  $\Phi$  according to the formula:

$$\Phi = A_{Ni} / \sigma \cdot N \cdot \lambda \quad (2)$$

With:

N: number of atoms of  $^{58}Ni$  per milligram of natural Ni

$\sigma$ : mean activation cross section in  $cm^2$

$\lambda$ : decay constant of  $^{58}Co$  in  $seconde^{-1}$

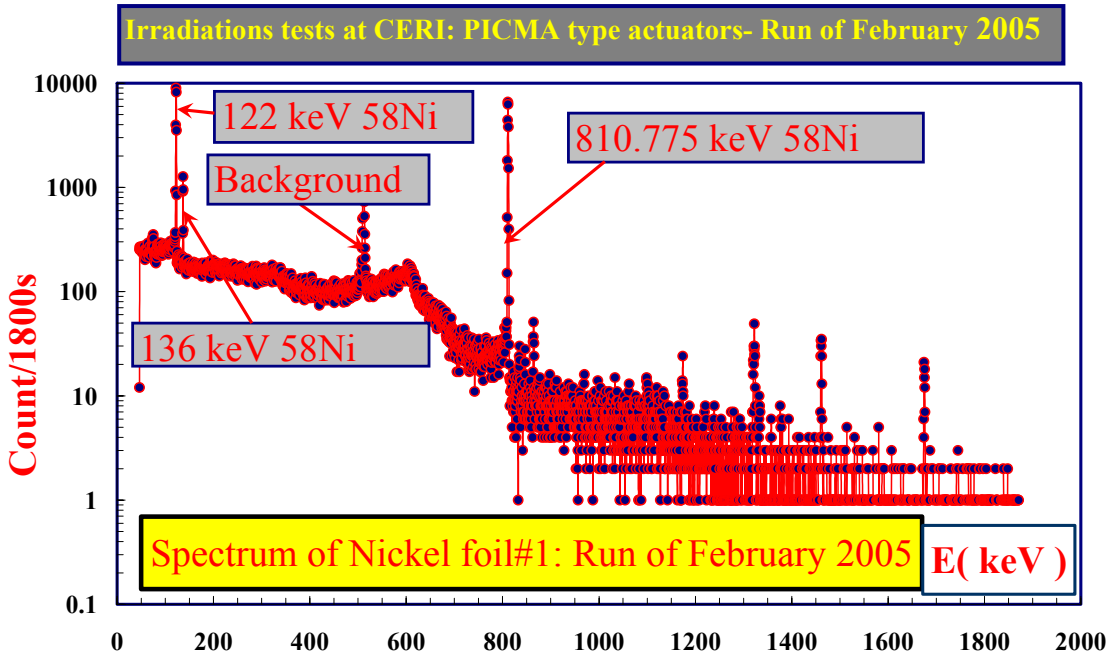


**Fig. 12: Typical spectrum of nickel foil #1 (Run of February 2005)**

Note that for the calculations only  $^{58}Ni$  radioisotope, which represents 68 % of natural nickel, is considered. Moreover the lifetime of  $^{58}Co$  is  $\tau = 70.864$  days leading to decay constant  $\lambda$  ( $\lambda = Ln 2 / \tau$ ) of  $1.13 \times 10^{-7}$   $seconde^{-1}$ . The values of the different parameters used in our calculations are given in Table 5.

N	$\sigma$ (cm <sup>2</sup> )	$\lambda$ (sec <sup>-1</sup> )
$7 \times 10^{18}$	$3.77 \times 10^{-25}$	$1.13 \times 10^{-7}$

**Table 5: Values of the different parameters of the fluence calculations**

**First experiment: PICMA piezoelectric actuators irradiations**

The irradiation tests with fast neutrons of four PICMA actuators, at liquid helium temperature were performed during two days: 16<sup>th</sup> and the 17<sup>th</sup> of February 2005. For this test, the distance between the beryllium target and the piezoelectric actuators vertical mid plane is 25 cm. Each of the sixteen nickel foils was analyzed after 18 days and we obtained the neutron fluence map shown in Fig. 13.

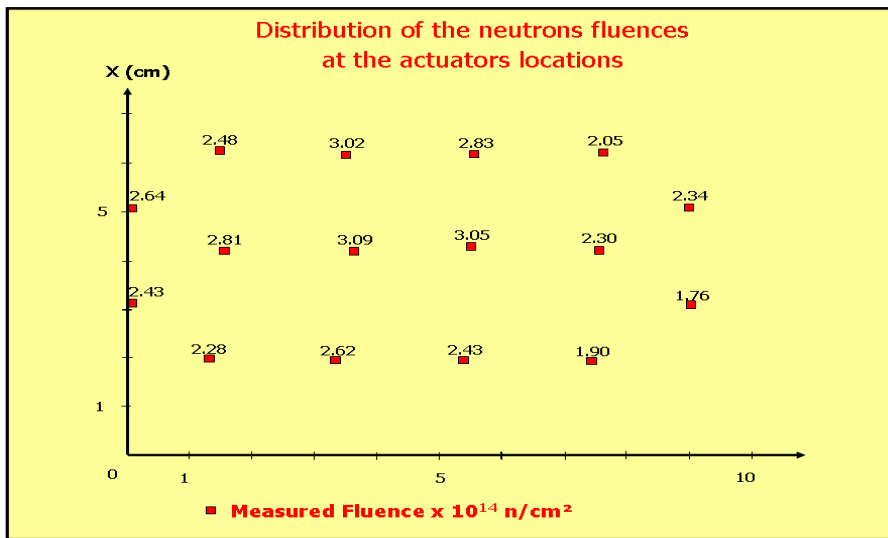


**Fig. 13: Neutrons fluence map for PICMA actuators irradiation**

It might be stressed that during irradiation test the nickel foils # 13-14-15-16 were fallen, however the corresponding data are consistent with those of the other foils. The corresponding distribution is illustrated in Fig. 4. The histogram shows a relatively uniform fluence distribution: the mean value is  $2.5 \times 10^{14}$  n/cm<sup>2</sup> with a standard deviation of  $\pm 16\%$ .

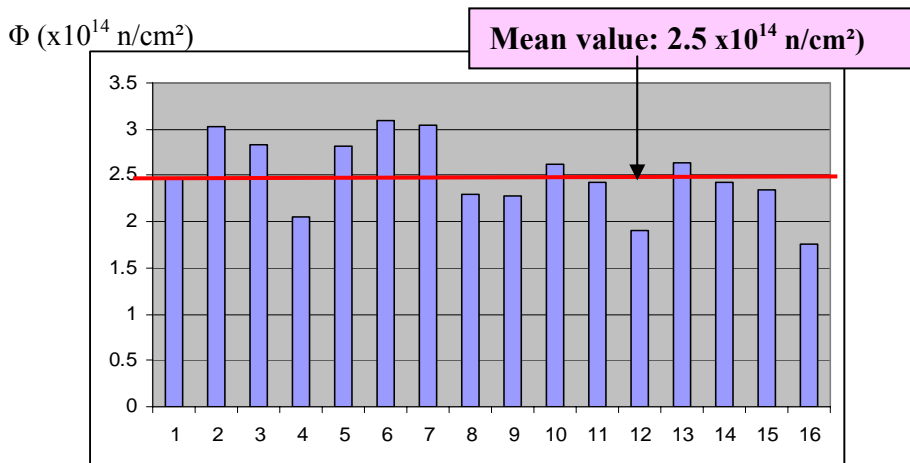


**Fig. 14: Neutrons fluence distribution for PICMA actuators irradiation**

## Second experiment: NOLIAC piezoelectric actuators irradiations

The second irradiation runs with fast neutrons of four NOLIAC actuators, at liquid helium temperature was performed during the 16<sup>th</sup> and the 17<sup>th</sup> of March 2005. In order to obtain higher neutron fluence as compared to the previous test, the distance between the beryllium target and the piezoelectric actuators vertical mid plane was reduced to 20 cm. Moreover, we also measure the slow neutrons fluence with activation of Au foils (Fig. 15). The measured distribution is shown in Fig. 16.

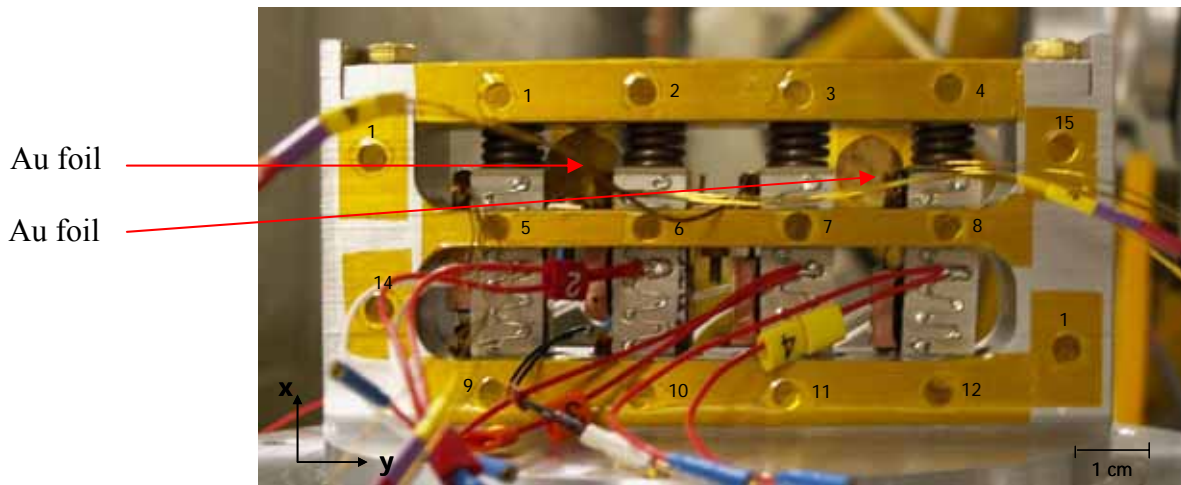


**Fig. 15: Distribution of the nickel foils on the NOLIAC piezoelectric actuators support**

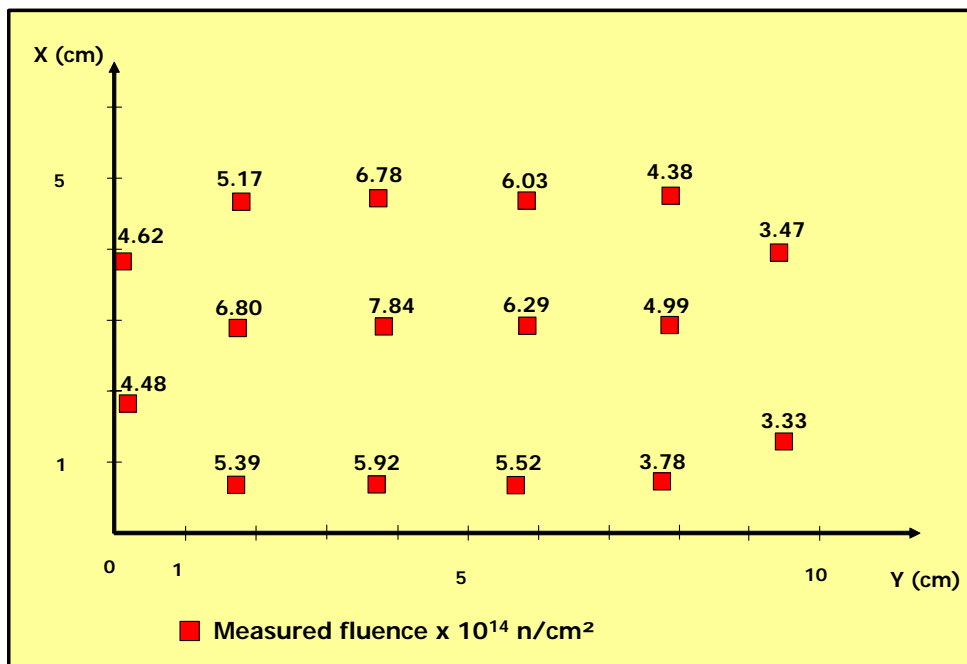


**Fig. 16: Neutron fluences distribution for NOLIAC actuators irradiation**

Notice again that during irradiation tests, nickel foils # 13-14-16 were fallen (even with double layer of kapton film) but the corresponding fluences at their locations are consistent with the data in other regions. The corresponding distribution is illustrated in Fig. 7. The histogram shows a relatively uniform fluence distribution: the mean value is  $5.3 \cdot 10^{14} \text{ n/cm}^2$  with a standard deviation of  $\pm 24\%$ . Our calculations for the slow neutrons fluence (energy range of 0.025 to  $10^6 \text{ eV}$ ) give  $2.423 \cdot 10^7 \text{ n/cm}^2/\text{s}$ . Some neutron fluences measurements have also been performed on the cryostat at 35 cm from the target and we find around  $1 \cdot 10^{14} \text{ n/cm}^2$ .

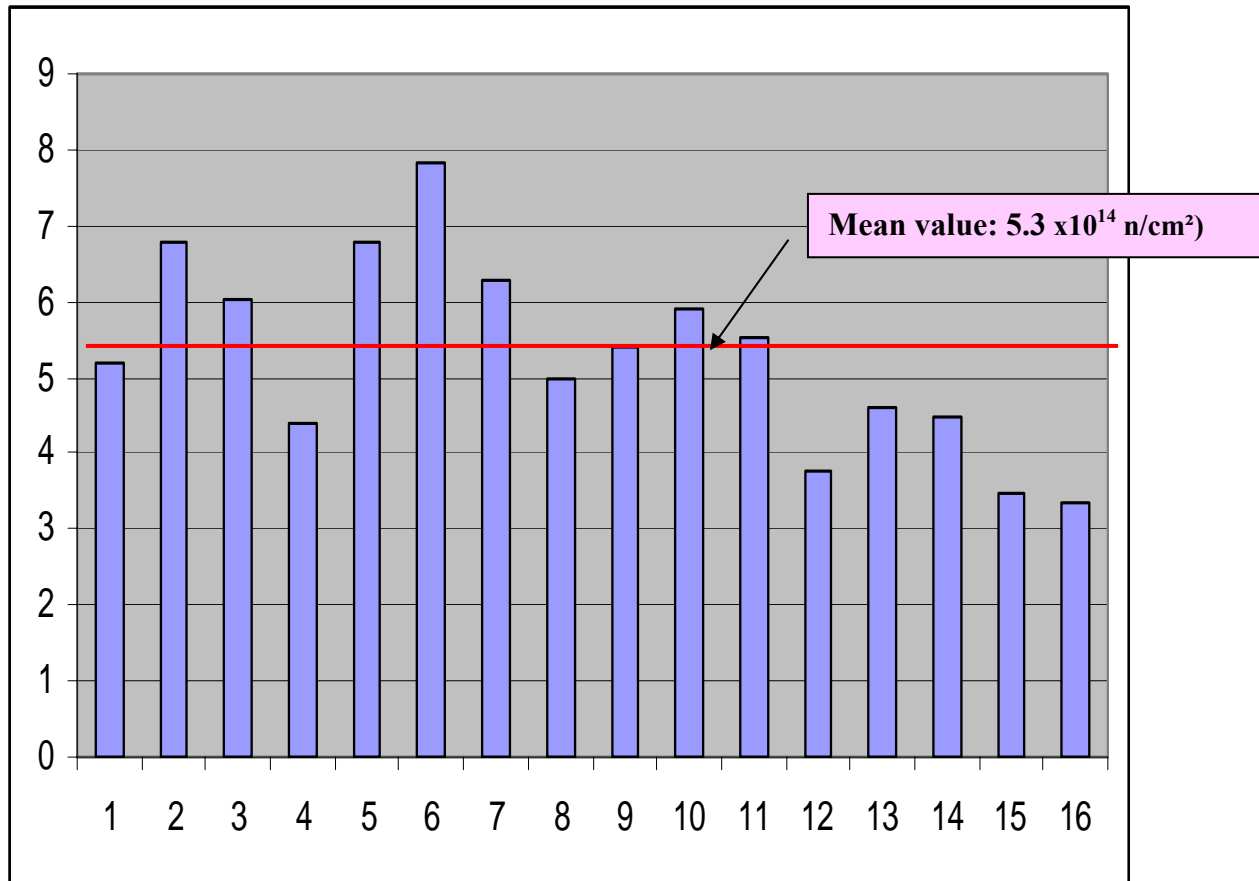


**Fig. 17: Neutrons fluence distribution for NOLIAC actuators irradiation**

We can notice that, by decreasing the distance between the target and the actuators by a factor 1.25, we increase the neutron fluence by a factor of 2.12.

### **Third experiment: JENA piezoelectric actuators irradiations**

The last irradiation campaign took place the 13<sup>th</sup> and the 14<sup>th</sup> of April 2005. The location of the nickel foils onto the Piezosystem JENA piezoelectric actuators support is shown in Fig.18. This picture was taken after irradiation and we can see that nickel foils # 14-15-16 were fallen.



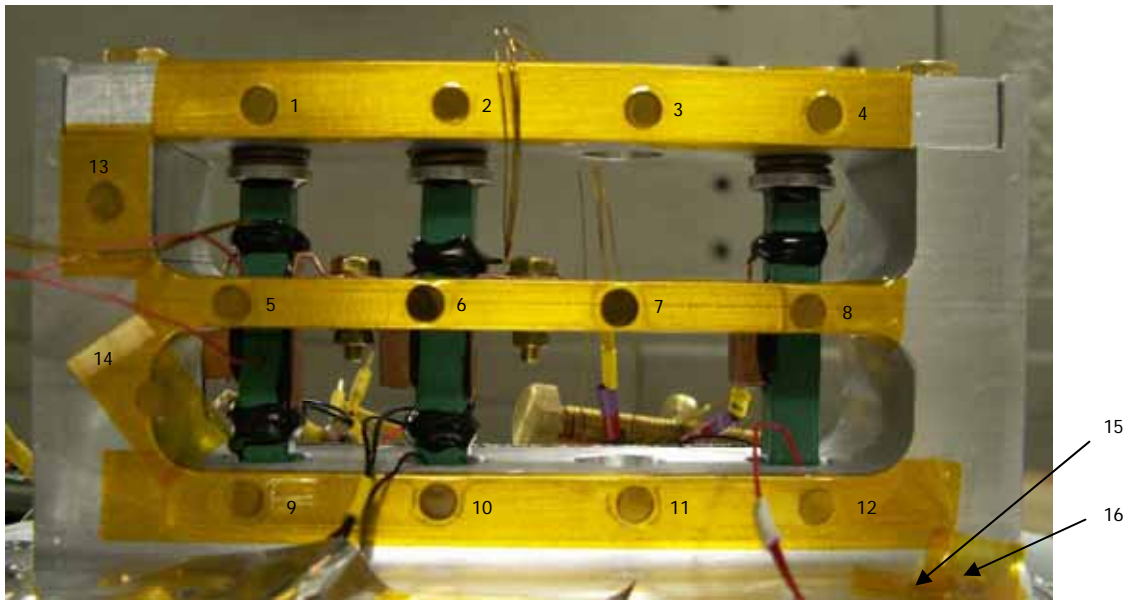


**Fig. 18: Distribution of the nickel foils on the JENA piezoelectric actuators support**

The distance Be target-piezoelectric actuators is always 20 cm. The analysis of the nickel foils leads to the neutron fluence map of Fig. 19.

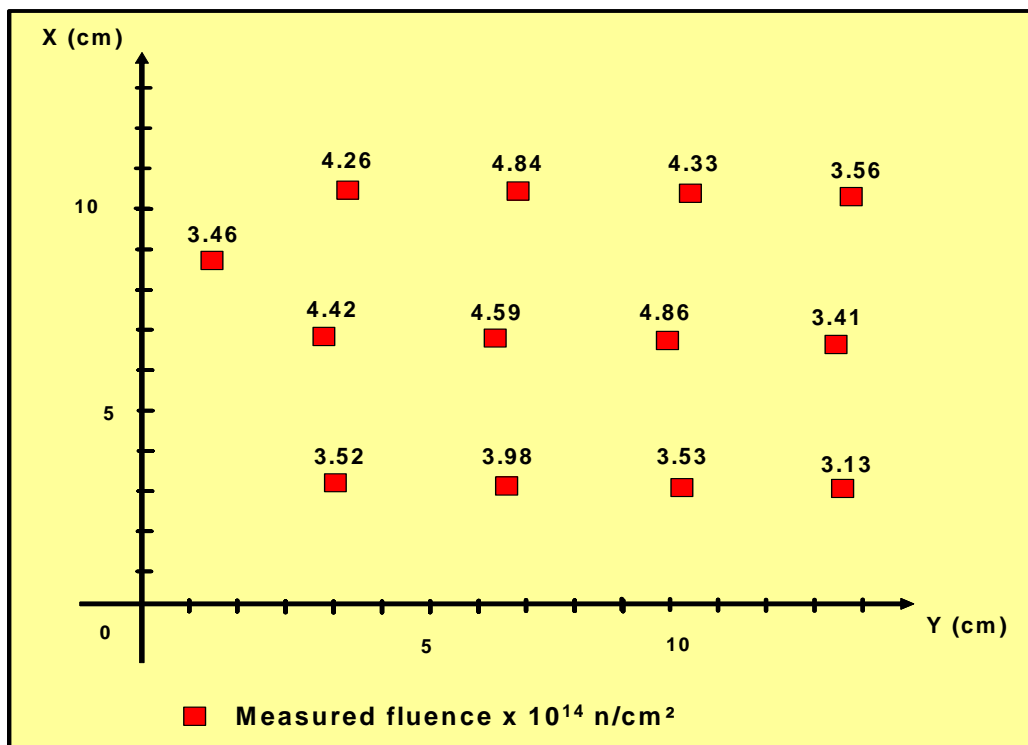


**Fig. 19: Neutron fluences distribution for JENA actuators irradiation**

The corresponding distribution is illustrated by the histogram in Fig. 20. The mean value is  $4.0 \cdot 10^{14} \text{ n/cm}^2$  with a standard deviation of  $\pm 15\%$ .

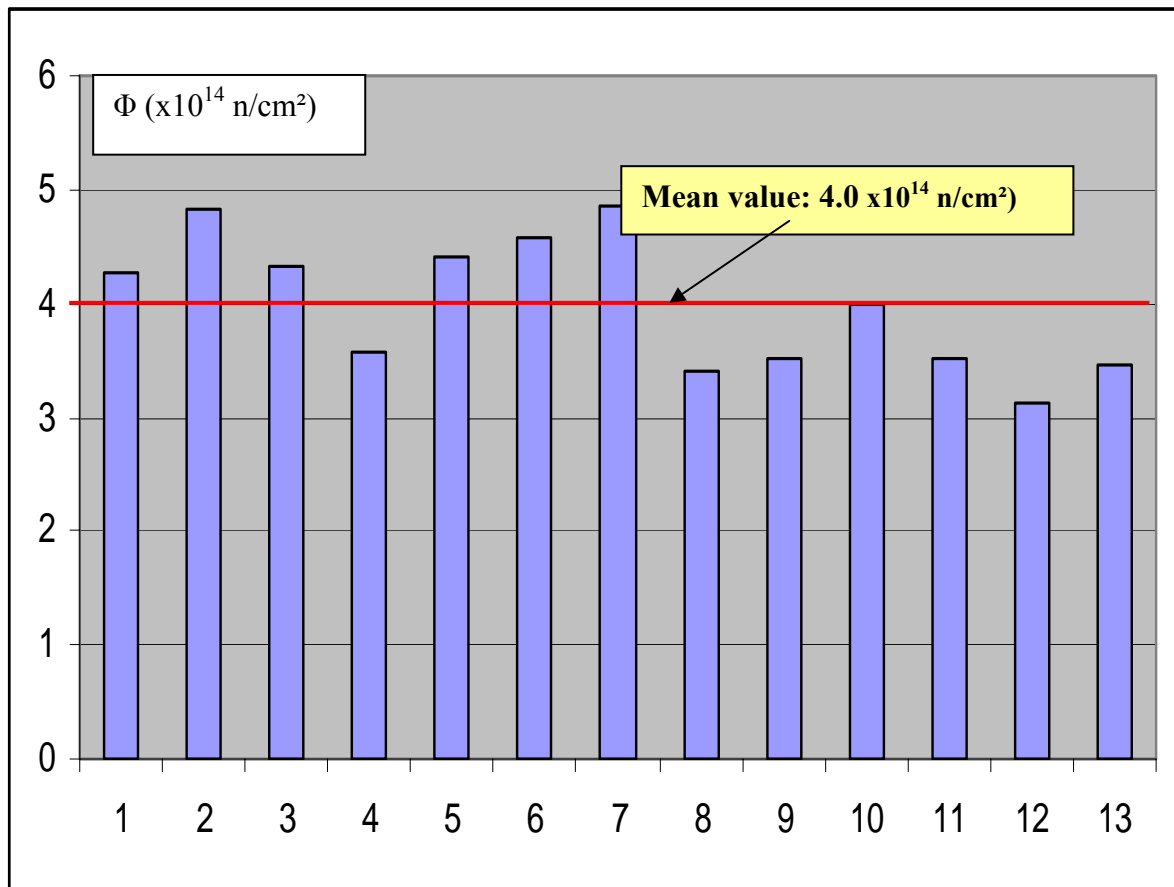


**Fig. 20: Neutrons fluence distribution for JENA actuators irradiation**

It should be emphasized that for Piezosystem JENA actuators, the neutron fluence is much lower than that observed for the test of NOLIAC actuators. This difference is mainly due to exposure durations, which are quite different: the durations of irradiation are 71880 s and 63900s for NOLIAC and Piezosystem JENA actuators respectively.

## Effects of fast neutrons on actuators electromechanical properties

After cool down to  $T=4.2\text{K}$ , the dielectric properties are measured without beam prior to radiation tests. Then, the actuators are subjected to fast neutrons radiation during  $\sim 20$  hours and the dielectric properties, the temperatures of the piezostacks as well as beam parameters are on-line measured while the test-cell is maintained at 4.2K: the beryllium target is bombarded by the deuteron beam, the current of which is increased progressively from  $1\ \mu\text{A}$  to  $35\ \mu\text{A}$ . Finally, the dielectric properties measured after neutron exposure to a dose higher than  $10^{14}$  neutrons/cm<sup>2</sup>, are compared to the reference values before radiation. As we have seen in a previous section, three beam tests were performed: four PICMA actuators in test #1, four NOLIAC actuators in test #2 and three Piezosystem JENA actuators for test #3. Notice that due to heating by neutrons beam, some parameters (e.g.,  $C_p$ ) increases with beam intensity.

The experimental data for two out of the three beam tests performed are illustrated in Fig. 20- Fig. 21. Notice that for the data illustrated in Fig. 20- Fig. 21, the errors bars are calculated by considering the shift of Allen Bradley thermometers, which have been previously measured in a separate experiment [7-9].

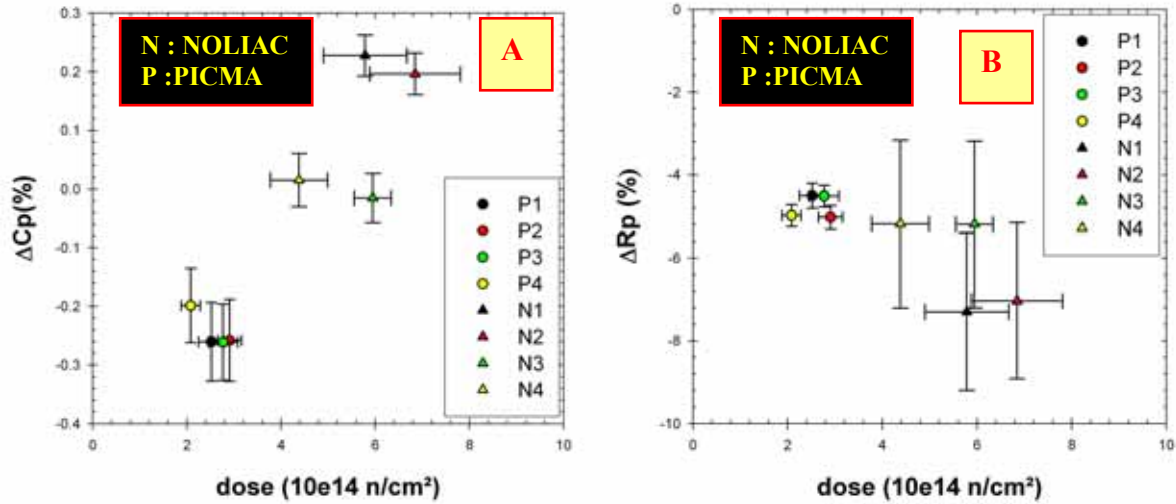


**Figure 20: Effect of fast neutrons dose on capacitance (A) and parallel resistance (B) at  $T=4.2$  K.**

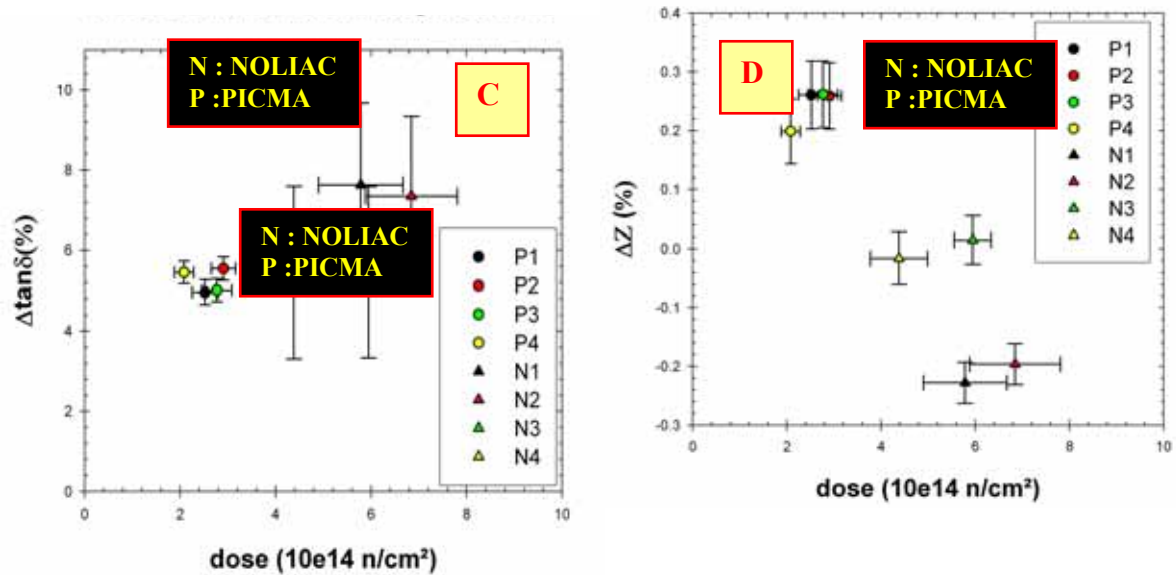


**Figure 21: Effect of fast neutrons dose on loss factor (C) and impedance (B).**

In the range of neutrons dose investigated ( $2- 7 \cdot 10^{14}$  n/cm<sup>2</sup>), the data call for the following remarks: 1) the capacitance of the actuators of PICMA type  $C_p$  decreases by 0.25% when the fast neutrons dose is increased, b) the capacitance of the actuators of NOLIAC type  $C_p$  increases by 0.15% when the fast neutrons dose is increased, 3) for the two type of piezostacks the loss factor increases by 5 to 10 % when the fast neutrons dose is increased.

In conclusion, no major damage was observed but slight performance degradation may be due to aging effect, is measured: these piezostacks are suited for use in cryogenic and neutrons radiation environment up to a total dose  $\sim 7.10^{14}$  n/cm<sup>2</sup>.

#### ACKNOWLEDGEMENT

We acknowledge the support of the European Community-Research Infrastructure Activity under the FP6 "Structuring the European Research Area" program (CARE, contract number RII3-CT-2003-506395)

#### REFERENCES

- 1 D. Edwards, 'Conceptual Design Report for the TESLA Test Facility', DESY Print, 1995.
- 2 J. Andruszkow et al., "TESLA The Superconducting Electron-Positron Linear Collider with an Integrated X-Ray Laser Laboratory- Technical Design Report, Part II : The Accelerator", Editors R.Brinkmann, K. Flöttmann, J.Rossbach, P. Schmüser, N. Walker, H. Weise, March 2001.
- 3 R. Brinkmann et al., 'TESLA XFEL, Technical Design Report Supplement', DESY 2002-167, 2002.
- 4 A. Gamp, 'On the preference of cold RF technology for the international linear collider', TESLA Report 2005-23, 2005.
- 5 A. Leuschner, S. Simrock, "Radiation field inside the tunnel of the linear collider TESLA", Laboratory Note, DESY D3-113, 2000.
- 6 J. Collot et al., NIM A 350 (1994), p. 525.
- 7 T. Junquera et al., 'Neutrons irradiation tests of calibrated cryogenic sensors at low temperature', Proc. CEC-ICMC' 97, 29 July- 1 August 1997, Portland, USA
- 8 J.F Amand et al., 'Neutron irradiation tests of pressure transducer in liquid helium', Proc. CEC-ICMC, 12-16 July 1999, Montreal, Canada
- 9 J.F Amand et al., 'Neutron irradiation tests in superfluid helium of LHC cryogenic thermometers', Proc. ICEC17, 14-17 July 1998, Bournemouth, UK
- 10 J. C Parnell Br. J. Radiol., 45 (1972) 542.
- 11 L. Maunoury, "Production de faisceaux d'ions radioactifs multi-chargés pour SPIRAL: études et réalisation du premier ensemble cible-source", PhD Thesis, Université de CAEN, GANIL T 98-01, 1998.